Enhanced Fluorescence of Remote Functionalized Diaminodicyanoquinodimethanes in the Solid State and Fluorescence Switching in a Doped Polymer by Solvent Vapors

S. Jayanty and T. P. Radhakrishnan*[a]

Abstract: Remote functionalized zwitterionic diaminodicyanoquinodimethanes are found to exhibit a dramatic enhancement of light emission in the solid state and when doped in polymer films, as compared to the solution state. Crystal structure analysis of prototypical molecules reveals the role of the remote functionality in the solid state molecular organization. Semiempirical quantum chemical computations provide a viable model to explain the interesting phenomenon of fluorescence enhancement as arising from the inhibition of geometry relaxation of the vertical excited state to a nonemitting state. The reversible switching of a doped polymer film fluorescence triggered by solvent vapors is demonstrated.

Keywords: diaminodicyanoquinodimethane · fluorescence enhancement · semiempirical calculations · solvent switch

Introduction

The strong fluorescence exhibited by most organic dye molecules in the monomeric state is quenched in the aggregated state. The current focus on the photoluminescence and electroluminescence of molecular materials provides impetus to explore novel chromophores which not only do not suffer fluorescence quenching in the aggregated state, but display enhanced light emission in the solid state and in polymer films. Only a few such cases have been reported. The superradiance observed in some thiacarbocyanine molecules has been attributed to dynamic energy transfer from the monomeric species to aggregate structures.[1] The highly emissive phase of a poly(*p*-phenyleneethynylene) was proposed to either arise from the metastable skewed chain alignments that allowed efficient interchain interactions or result from planarization effects.[2,3] Nano-sized aggregates of a sterically crowded silole[4] and a biphenyl substituted ethylene[5] have been reported to show strong light emission, presumably due to significant ground state conformational changes accompanying the aggregate formation. These reports suggest interesting and useful application potential in areas such as electroluminescence and sensors. However, detailed pictures of the physical origin of many of these observations are yet to emerge.

During our investigations of optical second harmonic generation in zwitterionic diaminodicyanoquinodimethanes (DADQ)[6–11] we have found that several molecules, especially the ones bearing remote functionalities[9–11] show enhanced fluorescence in the solid state compared to the solutions; similar effect was observed with these molecules doped in polymer films. Remote functionality refers to groups which are not in π-conjugation with the DADQ chromophore unit and therefore do not disturb the low lying electronic states of the chromophore. The role of viscous solvents and polymer matrices in enhancing the light emission of two related molecules have been investigated by Bloor et al.[12] Even though similar effects in solids were briefly noted, no detailed studies were presented or the impact of the molecular assembly in crystals analyzed. Further, these molecules do not possess remote functionalities involved in intermolecular noncovalent interactions, which as we will demonstrate below is a crucial feature in our systems. Our detailed investigation of the solution and solid state of a family of molecules and doped polymer films, establishes the generality of this interesting phenomenon and the molecular design principle involved. Zwitterionic DADQ's are prone to aggregation and the remote functionalities such as amino groups facilitate specific and directed intermolecular interactions promoting extended assembly. The remote groups appear to contribute positively to the

[a] S. Jayanty, Prof. T. P. Radhakrishnan
School of Chemistry, University of Hyderabad
Hyderabad, 500 046 (India)
Fax: (+91) 40-2301-2460
E-mail: tprsc@uohyd.ernet.in

Supporting information for this article is available on the WWW under http://www.chemeurj.org/ or from the author and contains the electronic absorption/emission of solutions of **1**–**8**, details of the crystal structures of **2** and **3**, summary of semiempirical computations (18 pages).

 DOI: 10.1002/chem.200305123

fluorescence enhancement since all the remote functionalized DADQ's we have examined exhibit this effect whereas many of the DADQ's without such functionality do not. More significantly, the presence of the remote groups imparts appreciable solubility to these molecules in water in addition to organic solvents. This is an important advantage since it facilitates convenient doping of these molecules in polymers which are soluble only in water enabling potential application in instances such as organic vapor sensing.

We have carried out a systematic investigation on a family of DADQ molecules with remote amino functionality including some in the form of salts (Figure 1); we present

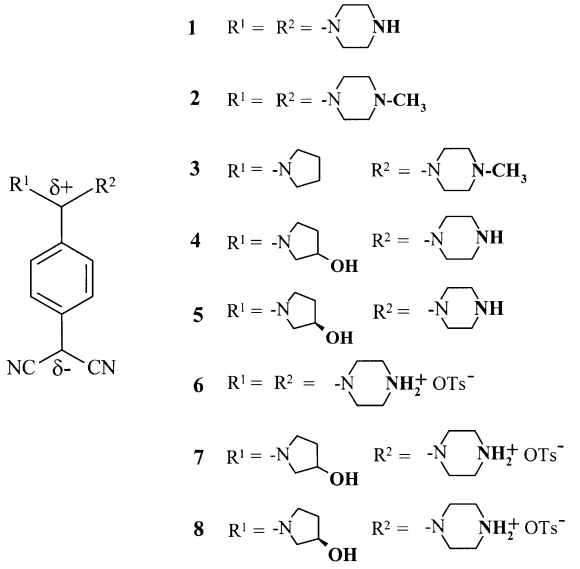

Figure 1. Molecules studied; the remote functionalities are in bold.

herein the salient findings which establish their enhanced fluorescence in the solid state and in polymer films. We also present crystal structures of prototypical systems and semi-empirical computational analysis of the molecular structure and energy in the ground and excited states leading to a simple model to explain this interesting phenomenon. A novel application potential of these materials is demonstrated through experiments on a chromophore doped in polymer film, showing reversible cycles of solvent vapor triggered fluorescence switching.

Results and Discussion

The family of molecules **1**–**8** exhibited fluorescence enhancement to varying extents in the crystalline state and in polymer films, compared with the solutions. We present the detailed results for **3** as an illustrative case and subsequently provide a summary of the observations for the whole family. The absorption and emission spectra of **3** in solvents of different polarity are shown in Figure 2a (see Experimental Section for details). The negative solvatochromism of the absorption spectra indicates the highly polar nature of the ground state of the molecule consistent with dipole moment measurements on similar molecules reported earlier.[13–15] The fluorescence quantum yield of **3** in acetonitrile solution estimated by comparison with quinine sulfate is only about 0.11%; this is typical of such molecules.[12] However, the solid sample as well as **3** doped in polymer films, polyvinyl alcohol (PVA) and poly(sodium 4-styrenesulfonate) (PSS) show bright green light emission when excited near their absorption peaks. The polymer films show clearly visible fluorescence even under ambient lighting. The spectra of **3** in the solid state and in polymer films are presented in Figure 2b. The strong enhancement of the emission compared with the solutions is evident from the normalized intensities. The absorption spectra in the solid state and in polymer films show similar linewidth and shape as the solution spectra, which indicates that the electronic states involved are molecular. Unlike the systems reported earlier,[2,3,5] molecular aggregation in the solid state appears to have little impact on the electronic absorption spectrum. This also implies that the extent of aggregation in the polymer films cannot be clearly established from the spectral data. The excitation spectra of the various cases, solution, solid and polymer films, show close resemblance to the absorption spectra suggesting that the emission is from the vertically excited state. The Stokes shifts observed are also within the range expected for vibrational relaxation alone of the excited state. The absorption and emission maxima of **1**–**8** in acetonitrile solution, solid state and polymer films are summarized in Table 1. The emission intensity of the various molecules in different solvents have the same order of magnitude, but as in the case of **3** (Figure 2a) the emission from low polar solvents are found to be slightly stronger than that from more polar solvents. The large enhancement of the normalized emission intensity in the solid state and in polymer films over the acetonitrile solution for the various com-

Table 1. Visible absorption (λ_{max}^{abs}) and emission (λ_{max}^{em}) peaks of **1**–**8** in acetonitrile solution, solid state and in PVA and PSS films and the ratio, *R* of the maximum intensity of the normalized emission in the solid and polymer films to that in acetonitrile solution.

Molecule	Acetonitrile solution	Solid		PVA film		PSS film	
	λ_{max}^{abs} [λ_{max}^{em}] /nm	λ_{max}^{abs} [λ_{max}^{em}] /nm	*R*	λ_{max}^{abs} [λ_{max}^{em}] /nm	*R*	λ_{max}^{abs} [λ_{max}^{em}] /nm	*R*
1	418 [539]	418 [525]	13	408 [526]	18	431 [543]	29
2	420 [543]	422 [492]	171	414 [514]	38	431 [536]	27
3	407 [538]	422 [495]	216	405 [505]	100	420 [527]	132
4	407 [533]	419 [534]	63	391 [514]	14	415 [526]	69
5	408 [539]	410 [553]	27	390 [510]	218	413 [524]	31
6	449 [549]	423 [526]	227	411 [509]	60	447 [547]	34
7	422 [540]	418 [518]	23	398 [518]	25	422 [528]	36
8	408 [536]	403 [531]	30	399 [523]	33	421 [525]	35

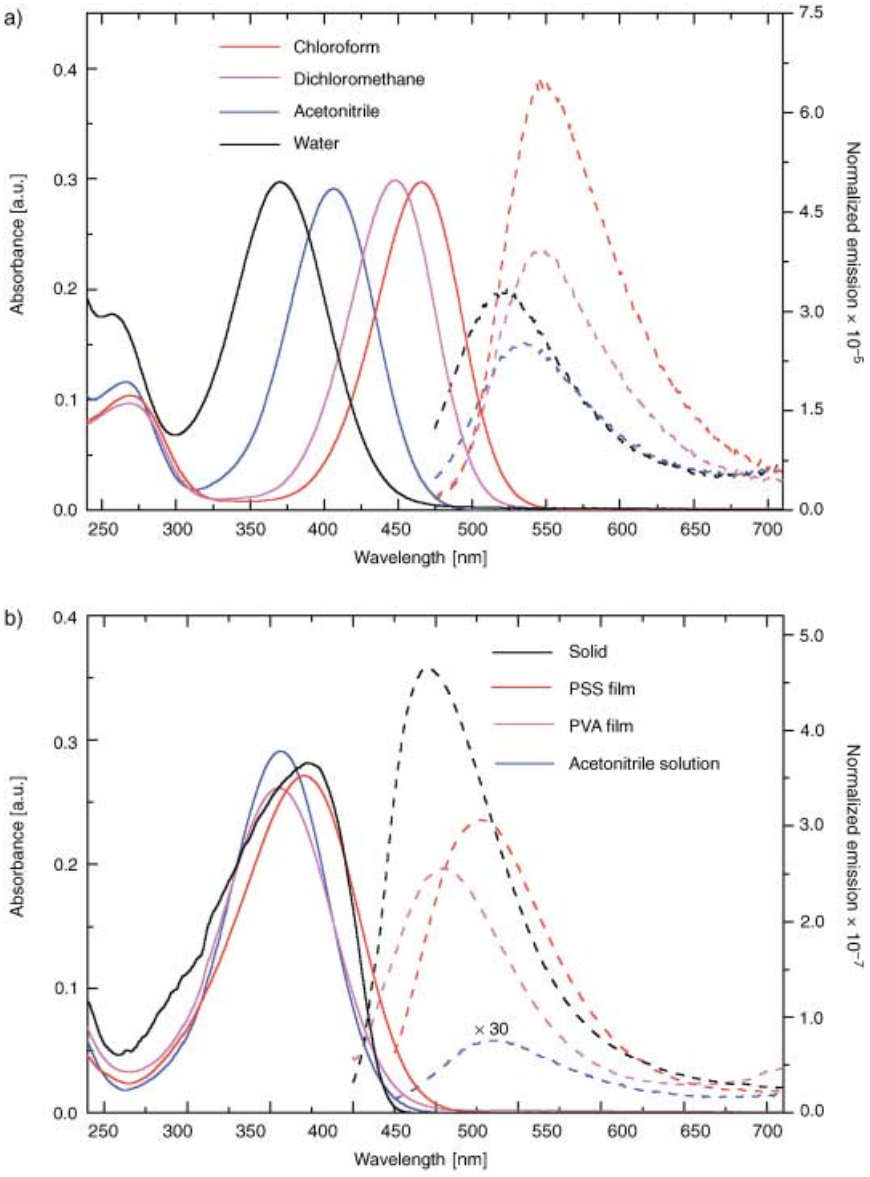

Figure 2. Absorption (——) and emission (-----) spectra of **3** a) in different solvents and b) in the solid state and polymer films (acetonitrile solution spectra with similar absorption λ_{max} are shown for comparison). The emission spectra are normalized by dividing by the optical density at λ_{max}; note the different scales in a) and b).

pounds are listed in Table 1 (the absorption λ_{max} of solids and doped polymer films are closest to that in acetonitrile than in other solvents); the enhancement factor, R ranges from 13 to 227. We note that the fluorescence intensities of the solids and doped polymer films measured may be less than the actual values due to factors such as self-absorption and wave-guiding. The latter is particularly relevant for polymer films where the light emission from the edges is not fully accounted for in the normal sample geometry employed. While these effects are difficult to quantify, the qualitative considerations indicate that the fluorescence enhancements we report for these materials are really their lower limits.

Deactivation of the chromophore excited state due to collisions with solvent molecules may contribute to the lower fluorescence observed in solutions. However, in view of the fact that in spite of such effects, most organic dye molecules exhibit stronger fluorescence in solution than in the solid state, one has to seek an explanation for the enhanced fluorescence observed in the present materials. Before embarking on an investigation of the origin of the fluorescence enhancement we have carried out single crystal X-ray structure analysis of **2** and **3** to gain insight into the molecular structure of these compounds and to explore the role of the remote functionality. The crystals are found to belong to the monoclinic space group, $P2_1/n$ and orthorhombic space group, *Pbca*, respectively.[16] The basic crystallographic data are presented in Table 2 and the molecular structures are shown in Figure 3.

Both molecules show a strong twist between the diaminomethylene unit and the benzenoid ring plane, a feature common among these molecules;[6–11,17] the dihedral angles, C2-C1-C7-N9 and C6-C1-C7-N10 are 52.6 and 53.5° in **2** and 50.6 and 53.0° in **3**, respectively. It should be noted that the situation is quite different from that in the case of the phenyleneethynylenes,[2,3] silole[4] and cyano-biphenylethylene[5] where the planar ground state conformation in the aggregates is considered to be an important factor contributing to the strong fluorescence. The bond lengths in the aromatic ring of **2** and **3** are typical of benzenoid structures and point to the zwitterionic nature of the molecules.[17] Examination of intermolecular contacts in these crystals reveals moderately close ones between the carbon atoms connected to the remote N atom of the piperazine units and the negatively polarized dicyanomethylene end of the zwitterionic diaminodicyanoquinodimethane moiety. The extended structure which results from such contacts in **2** and **3** are shown in Figure 4. Even though these noncovalent interactions are likely to be weak, their cooperative influence would steer the organization of the zwitterionic DADQ molecules and contribute to the enhanced tendency of these remote functionalized molecules towards aggregate formation. Strong intermolecular hydrogen-bond interactions mediated by the remote groups have been observed in **6**[11] and a derivative of **4** and **5**[7] in earlier studies. All these

Table 2. Basic crystallographic data for **2** and **3**.

	2	**3**
formula	$C_{20}H_{26}N_6$	$C_{19}H_{23}N_5$
F_w	350.47	321.42
crystal system	monoclinic	orthorhombic
space group	$P2_1/n$ (No. 14)	*Pbca* (No. 61)
color/appearance	yellow plate	yellow plate
dimensions [mm^3]	$0.64\times0.64\times0.36$	$0.52\times0.32\times0.24$
a [Å]	8.581(3)	16.32(7)
b [Å]	20.157(3)	12.400(17)
c [Å]	11.4040(13)	18.13(2)
β [°]	90.085(18)	90.0
Z	4	8
μ [cm^{-1}]	0.74	0.72
T [K]	293 (2)	293 (2)
λ [Å]	0.71703	0.71703
no. refls with $I\geq2\sigma_I$	3080	4597
no. parameters	235	217
GOF	0.992	0.983
R [for $I\geq2\sigma_I$]	0.0429	0.0550
wR^2 [for $I\geq2\sigma_I$]	0.1085	0.2374

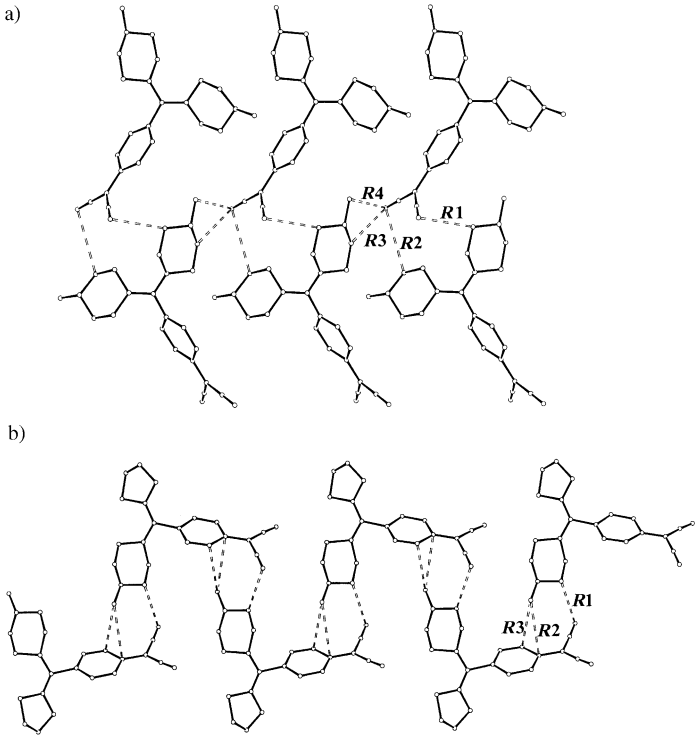

Figure 4. Intermolecular contacts (broken lines) leading to tape structures in a) **2** (extending along the crystallographic a axis; $R1=3.399$, $R2=3.564$, $R3=3.711$, $R4=3.787$ Å) and b) **3** (extending along the crystallographic b axis; $R1=3.698$, $R2=3.760$, $R3=3.897$ Å).

molecular associations are likely to play a significant role in obstructing the excited state conformational relaxation discussed below.

In order to investigate the likely molecular structure in solution, we have optimized the geometry of **3** using the AM1 method.[18] The molecular structure from crystal analysis served as a convenient starting point for the optimization and the solvent environment was modeled by invoking the COSMO subroutine.[19] As demonstrated earlier,[11,20–22] the same approach can be used to model the impact of the molecular environment in the solid state as well. Similar to our observation on related molecules,[11] the molecular twist, θ of the optimized ground state geometry of **3** is found to increase with the dielectric constant, ε employed in the computation; it increases from 39.8° at $\varepsilon=1$ and saturates at a value of about 66° at $\varepsilon>40$. The θ observed in the crystal is obtained when ε is in the range 2–4. CI calculations on the optimized ground state geometry provided the excitation energies. The enthalpy of formation of the ground state and the lowest vertical excited state at different ε are shown in Figure 5.

The computed λ_{max} agree very well with those observed for low polar solvents like dichloromethane and chloroform

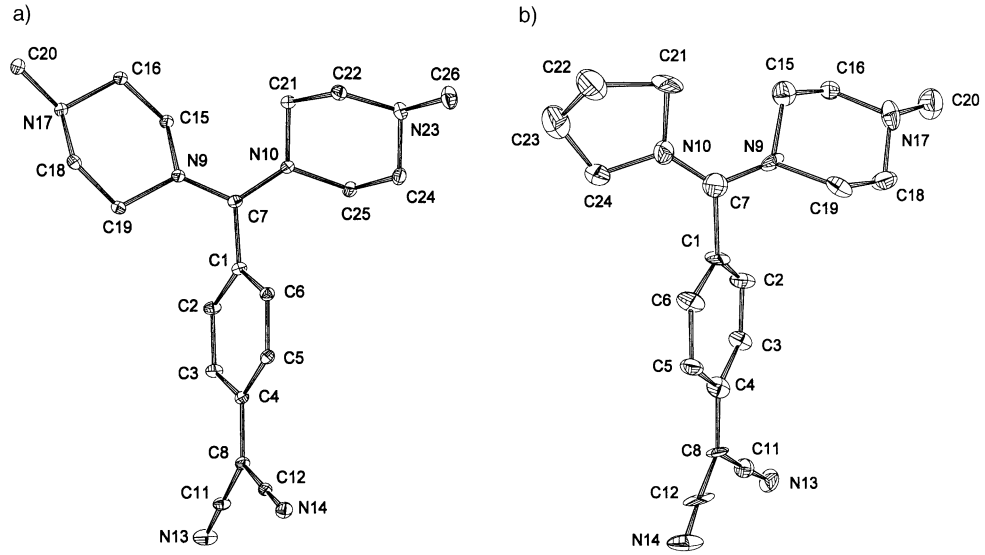

Figure 3. Molecular structure of a) **2** and b) **3** from single crystal X-ray analysis. 10% probability thermal ellipsoids are indicated and hydrogen atoms are omitted for clarity.

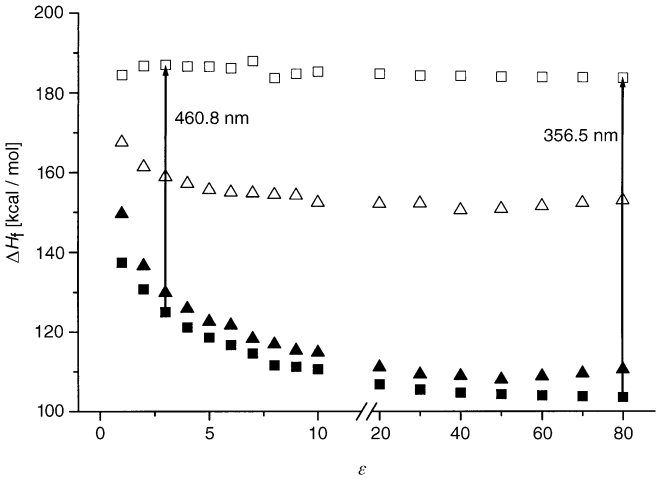

Figure 5. AM1/CI calculated enthalpy of formation at different ε, of **3** in the optimized ground state, the lowest vertical excited state, the optimized excited state and the ground state of the optimized excited state: ■ optimized ground state, □ vertical excited state, △ optimized excited state, ▲ ground state of optimized excited state.

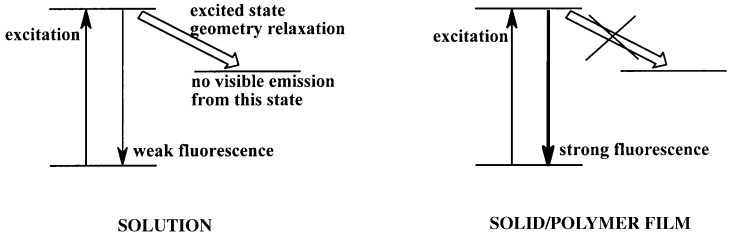

Figure 6. Schematic diagram illustrating the mechanism of fluorescence enhancement of diaminodicyanoquinodimethanes in the solid state and doped polymer films.

as well as the highly polar solvent, water. The λ_{max} at $\varepsilon = 4$ is in good agreement with the experimental value in the solid state. As noted earlier, the observed emission is likely to be from the vertical excited state alone. Even though geometry relaxation of the excited state is unlikely in the rigid solid state or polymer matrix, it is quite feasible in the solution state. In order to investigate the likely geometry relaxation, we have optimized the excited state structure under different ε values. The conspicuous change is the increase of θ to ~90° in all cases. The enthalpy of formation of these optimized geometries are plotted in Figure 5. The Figure also shows the enthalpy of formation of the ground states of these geometries from which we can estimate the upper bound for the emission energies of these relaxed geometries. The values are found to be in the range, 1588–673 nm (for ε ranging from 1–80), very much smaller than the observed emission energies suggesting that no visible light emission from the relaxed excited state geometries is observed in the solution, solid or polymer film. These computational results combined with the experimental facts noted earlier lead us to the conclusion that the enhancement of the fluorescence in the solid state and polymer films arise as a result of arresting the geometry relaxation of the excited fluorescent state to a nonfluorescent state. Conversely, geometry relaxation of the excited state leads to diminished fluorescence in solutions (Figure 6). Both excited state geometries are twisted and the difference is the extent of twisting; this situation may be contrasted with TICT systems[23] wherein planar and twisted geometries are considered. The current model is consistent with the qualitative picture proposed earlier for the matrix dependence of light emission from similar molecules.[12] It is important to note that in the model we develop for the DADQ's, the role of molecular aggregation is to facilitate further, the inhibition of excited state structure relaxation, rather than to force any kind of ground state geometry changes as implied in the models put forward in the case of the systems reported earlier.[3–5] In the polymer films, the structure relaxation would be hindered either by the rigidity of the polymer matrix or the aggregate formation, depending on the extent of aggregation. The energy gap between the vertical and relaxed excited states increases with ε (Figure 5) suggesting that, as the polarity of the solvent environment increases, the relative population of molecules in the vertical excited state would diminish progressively leading to reduction of fluorescence intensity; this is in agreement with the emission spectra observed in solution (Figure 2a). Future investigations would target the excited state dynamics in solution, solid and doped polymer states and their temperature dependence to gain further insight into the mechanism we have presented.

In order to examine the application potential of the fluorescence enhancement phenomenon, we have carried out an experiment on PVA films containing **3**, by alternately exposing it to chloroform vapors and drying. The fluorescence intensity of the film showed a clear reduction when it was enveloped by chloroform vapors emanating from the solvent placed at the bottom of the spectrometer cuvette. When the chloroform was removed and the film dried free of the vapors, the original fluorescence intensity was nearly regained (Figure 7). Two subsequent cycles showed stronger reduction of the fluorescence in presence of the vapors and

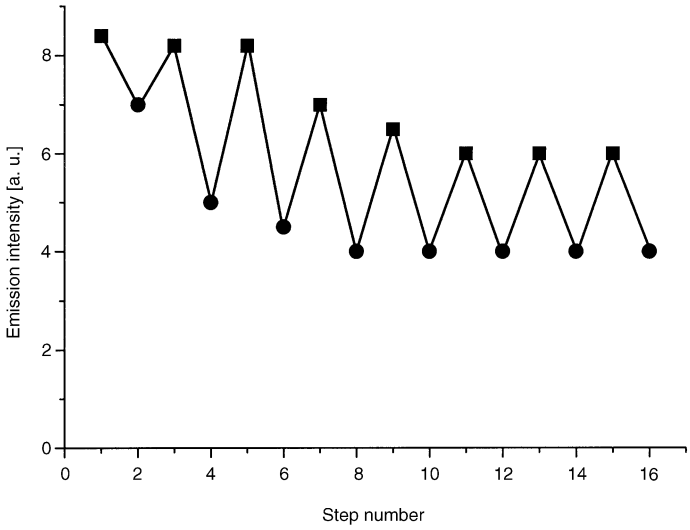

Figure 7. The variation of emission maximum (at 505 nm) of **3** in PVA film on exposure to chloroform vapors and subsequent drying, through consecutive steps: ■ on drying, ● on exposure to chloroform.

return to higher fluorescence in the dry state. Some change in the dry state fluorescence was observed during the initial cycles. The values stabilized subsequently and good reversibility was attained. At this stage, the reduction of fluorescence due to the vapors is quite substantial (~33%). Since the PVA matrix does not dissolve in chloroform and absolutely no leaching of the compound is observed throughout, we believe that the solvent vapors diffuse into the film and possibly cause local dissolution of part of the compound leading to fluorescence reduction. On drying, solid aggregates may be reformed recovering the enhanced fluorescence. Alternatively, a mild softening of the PVA matrix induced by the solvent vapor may facilitate structure relaxation and fluorescence quenching, which is reversed on drying. The present study provides a quantitative demonstration of the reversibility and repeatability of solvent vapor induced switching of the enhanced fluorescence in a chromophore doped polymer film.

Conclusion

We have explored a family of zwitterionic diaminodicyanoquinodimethanes and demonstrated enhanced light emission from them in the solid state and polymer films. The utility of the remote functionality in promoting molecular assembly is revealed by the crystallographic investigation of two of the molecules. A viable mechanism for the fluorescence enhancement is proposed through semiempirical computational analysis of the ground and excited state geometries and energies. We believe that such analysis may prove useful in understanding the basis for similar observations in other molecules reported previously. Experimental demonstration of reversible fluorescence switching triggered by solvent vapors is presented. These materials provide an ideal testing ground for the fascinating and relatively rare phenomenon of light emission enhancement in aggregates and are potential candidates for the development of novel photonic devices based on such phenomena.

Experimental and Computational Section

Synthesis and characterization

Compounds **1–8** were prepared using minor modifications of procedures reported[6–8,24] for similar molecules. Three typical cases are described below.

7,7-Bis(*N*-methylpiperazino)-8,8-dicyanoquinodimethane (2): *N*-Methylpiperazine (0.34 g, 3.4 mmol) was added to a warm solution of TCNQ (0.30 g, 1.47 mmol) in acetonitrile (30 mL) (CAUTION: HCN is a by-product). The solution turned dark green immediately and changed to yellow subsequently. Yellow crystalline product formed in about 1 h. The reaction mixture was stirred for 1.5 h more at 75 °C. The precipitate was filtered and dried (0.39 g, 82%).

7-(*N*-Methylpiperazino)-7-pyrrolidino-8,8-dicyanoquinodimethane (3): Pyrrolidine (0.094 g, 1.32 mmol) was added to a warm solution of TCNQ (0.30 g, 1.47 mmol) in acetonitrile (30 mL). The solution turned purple immediately and a purple crystalline compound precipitated in 1 h. The reaction mixture was stirred for 1.5 h more at 75 °C. The precipitate of 7-pyrrolidino-7,8,8-tricyanoquinodimethane, PTCNQ was filtered and dried (0.305 g, 83%). *N*-Methylpiperazine (0.12 g, 1.2 mmol) was added to a warm solution of PTCNQ (0.20 g, 0.98 mmol) in acetonitrile (20 mL) and the solution was stirred at 70 °C for 0.5 h and then at 30 °C for 1 h. Yellowish green fluorescent precipitate of **3** which separated out was filtered and dried (0.21 g, 81%).

7-(3-*R*-(+)-Hydroxypyrrolidino)-7-(piperazino)-8,8-dicyanoquinodimethane *p*-toluenesulfonate (8): Compound **5** was synthesized following similar procedure as for **3**. A solution of *p*-toluenesulfonic (PTS) acid (0.175 g, 1 mmol) in acetonitrile (5 mL) was added to a solution of **5** (0.25 g, 0.73 mmol) in acetonitrile (50 mL). The yellow microcrystalline powder of the PTS salt, **8** which precipitated out immediately was filtered and dried (0.307 g, 77%).

Characterization including single crystal structure of **1**[25] and **6**[11] have been reported earlier. The detailed characterization of the new compounds are provided below.

7,7-Bis(*N*-methylpiperazino)-8,8-dicyanoquinodimethane (2): Yield = 82%, recrystallized from acetonitrile; m.p. 278–280 °C (decomp); FTIR (KBr): $\tilde{\nu}$ = 2172.0, 2135.4, 1595.3 cm^{-1}; UV/Vis (acetonitrile): λ_{max} = 269, 420 nm; ^{1}H NMR ($CDCl_3$): δ = 1.7 (s, 6H), 2.6–2.7 (m, 8H), 3.5–3.6 (m, 8H), 7.1 ppm (s, 4H); ^{13}C NMR ([D$_6$]DMSO): δ = 34.5, 45.5, 50.9, 54.6, 114.1, 118.1, 123.2, 131.8, 149.8, 168.8 ppm; elemental analysis (%) calcd for $C_{20}H_{26}N_6$: C 68.57, H 7.43, N 24.00; found: C 68.31, H 7.11, N 24.61.

7-(*N*-Methylpiperazino)-7-pyrrolidino-8,8-dicyanoquinodimethane (3): Yield = 75%; recrystallized from acetonitrile; m.p. 260–262 °C (decomp); FTIR (KBr): $\tilde{\nu}$ = 2941.7, 2170.1, 2133.5, 1595.3 cm^{-1}, UV/Vis (acetonitrile): λ_{max} = 267, 407 nm; ^{1}H NMR ($CDCl_3$): δ = 1.6 (s, 3H), 2.0–2.1 (t, 4H), 2.15–2.25 (t, 4H), 3.5–3.6 (t, 4H), 3.60–3.75 (t, 4H), 7.0 ppm (s, 4H); ^{13}C NMR ([D$_6$]DMSO): δ = 24.1, 25.7, 33.1, 45.5, 50.1, 52.7, 54.6, 115.2, 118.1, 123.7, 130.5, 148.3, 165.9 ppm; elemental analysis (%) calcd for $C_{19}H_{23}N_5$: C 71.03, H 7.17, N 21.80; found: C 70.93, H 7.22, N 21.72.

7-(3-Hydroxypyrrolidino)-7-piperazino-8,8-dicyanoquinodimethane (4): Yield = 75%; recrystallized from acetonitrile/methanol; m.p. 245–246 °C (decomp); FTIR (KBr): $\tilde{\nu}$ = 3390.0, 2170.1, 2131.5, 1597.2 cm^{-1}; UV/Vis (acetonitrile): λ_{max} = 273, 407 nm; ^{1}H NMR ([D$_6$]DMSO): δ = 1.9–2.1 (m, 3H), 2.75–2.90 (m, 4H), 3.7–3.8 (m, 4H), 4.3–4.4 (m, 4H), 5.3 (s, 1H), 6.8–6.9 (d, 2H), 7.15–7.20 ppm (d, 2H), hydroxy proton was not observed; ^{13}C NMR ([D$_6$]DMSO): δ = 32.5, 33.1, 34.2, 46.1, 50.6, 51.8, 60.3, 67.6, 69.1, 115.1, 118.1, 123.8, 130.6, 148.3, 166.5 ppm; elemental analysis (%) calcd for $C_{18}H_{21}N_5O$: C 66.87, H 6.50, N 21.67; found: C 66.86, H 6.49, N 21.68.

7-(3-*R*(+)-Hydroxypyrrolidino)-7-piperazino-8,8-dicyanoquinodimethane (5): Yield = 77%; recrystallized from acetonitrile/methanol; m.p. 213–215 °C (decomp); FTIR (KBr): $\tilde{\nu}$ = 3308.0, 2170.0, 2131.0, 1597.0 cm^{-1}; UV/Vis (acetonitrile): λ_{max} = 270, 408 nm; ^{1}H NMR ([D$_6$]DMSO): δ = 1.8–2.1 (m, 3H), 2.7–2.9 (m, 4H), 3.6–3.9 (m, 4H), 4.2–4.5 (t, 4H), 5.3 (s, 1H), 6.8–6.9 (d, 2H), 7.2–7.35 ppm (d, 2H), hydroxy proton was not observed; ^{13}C NMR ([D$_6$]DMSO): δ = 32.2, 33.0, 34.3, 46.0, 50.6, 51.7, 60.3, 68.0, 69.1, 115.1, 118.1, 123.8, 130.6, 148.3, 166.5 ppm; elemental analysis (%) calcd for $C_{18}H_{21}N_5O$: C 66.87, H 6.50, N 21.67; found: C 66.22, H 6.85, N 21.68.

7-(Hydroxypyrrolidino)-7-piperazino-8,8-dicyanoquinodimethane *p*-toluenesulfonate (7): Yield = 75%; recrystallized from acetonitrile/methanol; m.p. 250–255 °C (decomp); FTIR (KBr): $\tilde{\nu}$ = 3398.2, 3022.8, 2177.8, 2137.0, 1597.0, 1005.0, 887.0, 814.0 cm^{-1}; UV/Vis (acetonitrile): λ_{max} = 267, 422 nm; ^{1}H NMR ([D$_6$]DMSO): δ = 1.9–2.0 (m, 3H), 2.1–2.2 (m, 4H), 2.3 (s, 3H), 3.8–4.0 (m, 4H), 4.30–4.45 (t, 2H), 5.25–5.40 (m, 2H), 6.8–6.9 (m, 2H), 7.1–7.2 (d, 2H), 7.3–7.4 (m, 2H), 7.5–7.6 (d, 2H), 8.85–9.15 ppm (s, 2H), hydroxy proton was not observed; ^{13}C NMR ([D$_6$]DMSO): δ = 21.0, 32.5, 33.3, 34.0, 43.1, 44.7, 49.7, 50.8, 60.1, 60.6, 67.5, 69.1, 114.7, 118.1, 123.7, 125.7, 128.4, 130.7, 138.2, 145.5, 148.5, 167.0 ppm, the extra peaks additional to the number of symmetry nonequivalent atoms appears to result from clustering of these zwitterionic molecules, since we have verified their reproducibility and by repeated purification ensured that they are not due to any impurities which is further confirmed by the satisfactory elemental analysis; elemental analysis (%) calcd for $C_{25}H_{29}N_5SO_4$: C 60.61, H 5.86, N 14.14; found: C 60.62, H 5.89, N 14.24.

7-(3-*R*(+)-Hydroxypyrrolidino)-7-(piperazino)-8,8-dicyanoquinodimethane *p*-toluenesulfonate (8): Yield = 77%; recrystallized from acetonitrile/methanol; m.p. 239–244 °C (decomp); FTIR (KBr): $\tilde{\nu}$ = 3362.2, 3015.0, 2177.8, 2137.3, 1597.2, 1005.0, 887.3, 814.0 cm^{-1}; UV/Vis (acetonitrile): λ_{max} = 265, 408 nm; ^{1}H NMR ([D$_6$]DMSO): δ = 1.9–2.0 (m, 3H), 2.1–2.2 (m, 4H), 2.3 (s, 3H), 3.6–3.9 (m, 4H), 4.25–4.45 (m, 2H), 5.25–

5.40 (m, 2H), 6.8–6.9 (m, 2H), 7.1–7.2 (d, 2H), 7.25–7.4 (m, 2H), 7.5–7.6 (d, 2H), 8.8–9.2 ppm (s, 2H), hydroxy proton was not observed; ^{13}C NMR ([D$_6$]DMSO): δ = 21.0, 32.6, 33.7, 34.1, 43.0, 47.1, 50.7, 51.3, 60.0, 61.0, 67.6, 69.3, 114.5, 118.1, 123.6, 125.7, 128.4, 130.9, 138.4, 145.2, 148.8, 166.7 ppm, the extra peaks additional to the number of symmetry nonequivalent atoms appears to result from clustering of these zwitterionic molecules, since we have verified their reproducibility and by repeated purification ensured that they are not due to any impurities, which is further confirmed by the satisfactory elemental analysis; elemental analysis (%) calcd for $C_{25}H_{29}N_5SO_4$: C 60.61, H 5.86, N 14.14; found: C 60.55, H 5.93, N 14.21.

Preparation of doped polymer films

In the present study we have considered only water soluble polymers, PVA (M_W = 15000) and PSS (M_W = 70000), since we were interested in exploring the fluorescence response of the doped polymer films in presence of organic solvent vapors; however, these compounds can be incorporated in other polymers as well. Equal volumes of aqueous solutions of the compound (5 mM) and the polymer (~0.2 g mL^{-1}) were mixed and subjected to ultrasonication for 5 min. The films were prepared by spin casting on glass plates followed by drying in a vacuum desiccator and hot air oven at 80 °C for 1 h each.

Electronic spectroscopy

The electronic absorption spectra of solutions and doped polymer films were recorded on a Shimadzu UV/Vis spectrometer (Model UV-3101). The concentrations were adjusted to achieve an optical density of ~0.3 in all cases. The specular reflectance (8° incidence) spectrum of the solid compounds in the form of KBr pellets were recorded using the integrating sphere (ISR 3100) attachment of the spectrometer. The reflectance spectra were converted to absorption profiles using the Kubelka–Munk function. The weight ratio of the solid compound to KBr was adjusted in each case to achieve a final optical density of ~0.3. The emission spectra were recorded on a Jobin Yvon Horiba spectrofluorimeter (Model Fluoromax-3) by exciting approximately 10 nm below the absorption λ_{max}. The solid and polymer film samples were mounted diagonally in the standard cuvette so that the signal is detected at 90° to the exciting beam in the normal geometry used for fluorescence measurements in solution. The spectra are normalized by dividing by the optical density at λ_{max} of the same sample, so that a fair comparison can be made between the intensity of emission from solution, solid and polymer films.

Crystal structure determination

X-ray diffraction data were collected on an Enraf-Nonius MACH3 diffractometer. $Mo_{K\alpha}$ radiation with a graphite crystal monochromator in the incident beam was used. Data was reduced using Xtal3.4;[26] Lorentz and polarization corrections were included. All non-hydrogen atoms were found using the direct method analysis in SHELX-97[27] and refined anisotropically. After several cycles of refinement the positions of the hydrogen atoms were calculated and added to the refinement process. Graphics were handled using ORTEX6a.[28] In the case of **2**, the data were collected and structure solved under monoclinic P lattice; however the β angle deviates from 90° by only 0.085(18). Therefore we have examined the lattice transformation to orthorhombic *P*; however, the set of systematic absences found in the transformed reflection data is not compatible with any of the space groups in this Bravais lattice. Further, we have checked the symmetry of the Friedel pairs of several reflections; out of the four pairs in an (*hkl*) set, the intensity of reflection of two are distinctly different from (ranging from 2–50% of) the other two, indicating the monoclinic symmetry of the lattice. Detailed crystallographic data are submitted as Supporting Information.

Computations

Semiempirical quantum chemical computations were carried out using the MOPAC93 program package[29] using the AM1 method.[18] The geometry optimizations involved no constraints and the PRECISE option was employed. The microenvironment of the molecule was modeled using the COSMO subroutine[19] employing various dielectric constants in the range 1 to 80. The parameter, NSPA (number of segments per atom) was set equal to 60 in all calculations. Enthalpies of formation were computed following full configuration interaction (CI) calculation within the 6 molecular orbitals bracketing the HOMO/LUMO, involving the 400 singlet microstates. The computational results are presented in the Supporting Information.

Acknowledgement

Financial support from the Department of Science and Technology, New Delhi (Swarnajayanti Fellowship), the use of the National Single Crystal Diffractometer Facility funded by the DST at the School of Chemistry, University of Hyderabad and the "University with Potential for Excellence" program of the University Grants Commission, New Delhi are acknowledged. S.J. thanks the CSIR, New Delhi for a senior research fellowship. We thank Profs. M. Durga Prasad and A. Samanta for insightful discussions.

[1] S. Özcelik, D. L. Akins, *J. Phys. Chem. B* **1999**, *103*, 8926.
[2] R. Deans, J. Kim, M. R. Machacek, T. M. Swager, *J. Am. Chem. Soc.* **2000**, *122*, 8565.
[3] M. Levitus, K. Schmieder, H. Ricks, K. D. Shimizu, U. H. F. Bunz, M. A. Garcia-Garibay, *J. Am. Chem. Soc.* **2001**, *123*, 4259.
[4] J. Luo, Z. Xie, J. W. Y. Lam, L. Cheng, H. Chen, C. Qiu, H. S. Kwok, X. Zhan, Y. Liu, D. Zhu, B. Z. Tang, *Chem. Commun.* **2001**, 1740.
[5] B. An, S. Kwon, S. Jung, S. Y. Park, *J. Am. Chem. Soc.* **2002**, *124*, 14410.
[6] M. Ravi, D. N. Rao, S. Cohen, I. Agranat, T. P. Radhakrishnan, *Chem. Mater.* **1997**, *9*, 830.
[7] M. Ravi, P. Gangopadhyay, D. N. Rao, S. Cohen, I. Agranat, T. P. Radhakrishnan, *Chem. Mater.* **1998**, *10*, 2371.
[8] P. Gangopadhyay, S. Sharma, A. J. Rao, D. N. Rao, S. Cohen, I. Agranat, T. P. Radhakrishnan, *Chem. Mater.* **1999**, *11*, 466.
[9] S. Jayanty, T. P. Radhakrishnan, *Chem. Mater.* **2001**, *13*, 2072.
[10] S. Jayanty, P. Gangopadhyay, T. P. Radhakrishnan, *J. Mater. Chem.* **2002**, *12*, 2792.
[11] S. Jayanty, T. P. Radhakrishnan, *Chem. Mater.* **2001**, *13*, 2460.
[12] D. Bloor, Y. Kagawa, M. Szablewski, M. Ravi, S. J. Clark, G. H. Cross, L. Pålsson, A. Beeby, C. Parmer, G. Rumbles, *J. Mater. Chem.* **2001**, *11*, 3053.
[13] Y. Kagawa, M. Szablewski, M. Ravi, N. Hackman, G. H. Cross, D. Bloor, A. S. Batsanov, J. A. K. Howard, *Nonlinear Opt.* **1999**, *22*, 235.
[14] R. S. Gopalan, G. V. Kulkarni, M. Ravi, C. N. R. Rao, *New J. Chem.* **2001**, *25*, 1108.
[15] J. M. Cole, R. C. B. Copley, G. J. McIntyre, J. A. K. Howard, M. Szablewski, G. H. Cross, *Phys. Rev. B* **2002**, *65*, 125107.
[16] CCDC-206354 and -206355 contain the supplementary crystallographic data for this paper. These data can be obtained free of charge via www.ccdc.cam.ac.uk/conts/retrieving.html (or from the Cambridge Crystallographic Data Centre, 12, Union Road, Cambridge CB21EZ, UK; fax: (+44) 1223-336-033; or deposit@ccdc.cam.ac.uk).
[17] M. Ravi, T. P. Radhakrishnan, *J. Phys. Chem.* **1995**, *99*, 17624.
[18] M. J. S. Dewar, E. G. Zoebisch, E. F. Healy, J. J. P. Stewart, *J. Am. Chem. Soc.* **1985**, *107*, 3902.
[19] A. Klamt, G. Shüürmann, *J. Chem. Soc. Perkin Trans. 2* **1993**, 799.
[20] S. Sharma, T. P. Radhakrishnan, *J. Phys. Chem. B* **2000**, *104*, 10191.
[21] S. Sharma, T. P. Radhakrishnan, *J. Phys. Chem. B* **2003**, *107*, 147.
[22] S. Sharma, T. P. Radhakrishnan, *ChemPhysChem* **2003**, *4*, 67.
[23] a) W. Rettig, *Angew. Chem.* **1986**, *98*, 969; *Angew. Chem. Int. Ed. Engl.* **1986**, *25*, 971; b) K. Bhattacharyya, M. Chowdhury, *Chem. Rev.* **1993**, *93*, 507.
[24] L. R. Hertler, H. D. Hartzler, D. S. Acker, R. E. Benson, *J. Am. Chem. Soc.* **1962**, *84*, 3387.
[25] M. Ravi, S. Cohen, I. Agranat, T. P. Radhakrishnan, *Struct. Chem.* **1996**, *7*, 225.
[26] *Xtal 3.4*, (Eds.: S. R. Hall, G. S. D. King, J. M. Stewart), University of Western Australia, Perth (Australia), **1995**.
[27] G. M. Sheldrick, SHELX-97, University of Göttingen, Göttingen (Germany), **1997**.
[28] P. McArdle, *J. Appl. Crystallogr.* **1995**, *28*, 65.
[29] MOPAC93 Fujitsu Inc., Japan.

Received: May 9, 2003
Revised: July 4, 2003 [F5123]

